Available online at www.sciencedirect.com
SCIENCE DIRECT
Surface Science 600 (2006) 318–324
SURFACE SCIENCE
www.elsevier.com/locate/susc

Phosphorus and hydrogen atoms on the (001) surface of silicon: A comparative scanning tunnelling microscopy study of surface species with a single dangling bond

T.C.G. Reusch [a,*], N.J. Curson [a], S.R. Schofield [a,b], T. Hallam [a], M.Y. Simmons [a]

[a] Centre for Quantum Computer Technology, School of Physics, University of New South Wales, Sydney 2052, NSW, Australia
[b] School of Mathematical and Physical Sciences, The University of Newcastle, Callaghan 2308, NSW, Australia

Received 20 July 2005; accepted for publication 21 October 2005
Available online 28 November 2005

Abstract

We present a comparative scanning tunnelling microscopy (STM) study of two features on the Si(001) surface with a single dangling bond. One feature is the Si–P heterodimer—a single surface phosphorus atom substituted for one Si atom of a Si–Si dimer. The other feature is the Si–Si–H hemihydride—a single hydrogen atom adsorbed to one Si atom of a Si–Si dimer. Previous STM studies of both surface species have reported a nearly identical appearance in STM which has hampered an experimental distinction between them to date. Using voltage-dependent STM we are able to distinguish and identify both heterodimer and hemihydride on the Si(001) surface. This work is particularly relevant for the fabrication of atomic-scale Si:P devices by STM lithography on the hydrogen terminated Si(001):H surface, where it is important to monitor the distribution of single P dopants in the surface. Based on the experimental identification, we study the lateral P diffusion out of nanoscale reservoirs prepared by STM lithography.

Keywords: Scanning tunnelling microscopy; Nanopatterning; Surface diffusion; Silicon; Phosphorus; Hydrogen

1. Introduction

Currently there is growing interest in using a scanning tunnelling microscope (STM) to pattern surfaces [1] for the fabrication of devices with atomic-scale placement of phosphorus (P) dopants in silicon (Si). This technique has been proposed for building quantum cellular automata [2], single electron transistors [3–5], and a Si based quantum computer [6–9]. In these approaches, STM lithography is used to selectively desorb hydrogen from a hydrogen terminated Si(001):H surface from the nanometer down to the atomic scale. After dosing the patterned surface with phosphine (PH_3) gas, the PH_3 molecules are found to adsorb only to the exposed Si dangling bonds [10]. By subsequent annealing, the phosphorus atoms are then incorporated into the surface and the hydrogen resist layer is removed [10–12]. Recently, Schofield et al. demonstrated the positioning of single dopants in the surface with atomic precision [13]. Furthermore, it has been shown that nanoscale devices can be fabricated, encapsulated and contacted with conventional lithography by using a novel registration scheme [14].

A common but not well-known problem in fabricating Si:P devices by STM lithography is that two surface species are produced which appear very similar in STM imaging: the Si–P heterodimer (HD), and the Si–Si–H hemihydride (HH) (see Fig. 1). The HD is the result of an incorporation reaction in which a single P atom substitutes one Si atom of a Si–Si dimer in the (2×1) reconstructed Si(001) surface [11,12,15]. The HH consists of a single hydrogen atom adsorbed to one Si atom of a dimer [16]. In the context of the above device fabrication procedure, the HH arises from the non-perfect desorption of the hydrogen [17]. Furthermore, HH may be present even without deliberate hydrogen

* Corresponding author.
E-mail address: thilo.reusch@unsw.edu.au (T.C.G. Reusch).

0039-6028/$ - see front matter © 2005 Elsevier B.V. All rights reserved.
doi:10.1016/j.susc.2005.10.031

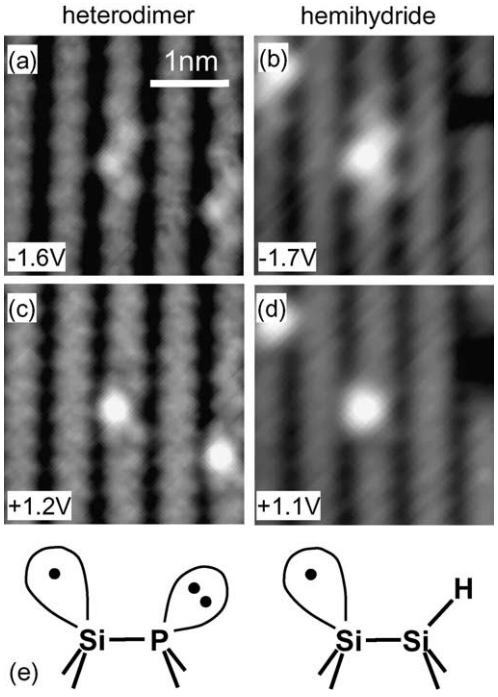

Fig. 1. STM topographies of the Si–P heterodimer and the Si–Si–H hemihydride. The left column shows a heterodimer in filled and empty states [(a) $U = -1.6$ V, (c) $U = +1.2$ V]. The right column depicts a hemihydride at similar biases [(b) $U = -1.7$ V, (d) $U = +1.1$ V]. Both features appear very similar. (e) Schematic diagrams of a Si–Si–P heterodimer and a H–Si–Si–H hemihydride.

dosing due to adsorption from the residual gas in ultra-high vacuum (UHV). The HD is of course the desired product of incorporating the P dopant into the surface layer.

Separate STM studies of both features have been reported previously [11,15,16,18–26]. From these studies it becomes obvious that both features appear very similar in STM imaging. Fig. 1 highlights this similarity, where we present voltage-dependent STM topographies obtained in our group in different experiments under nearly identical imaging conditions. The left column shows a HD imaged in filled (sample voltage $U < 0$) and empty ($U > 0$) electronic states, whereas the right hand side shows a HH at comparable biases. The schematic structure of both features is depicted at the bottom (Fig. 1(e)). Imaging the filled electronic states (Fig. 1(a) and (b)) shows that both features appear asymmetric with an elevation on one side of the dimer row as reported previously [11,15,16,18–26] and static buckling visible on the neighboring 2–3 dimers. In empty states imaging (Fig. 1(c) and (d)), both species appear asymmetric with an elevation on one side of the dimer row and a depression on the other side. The elevation in both filled and empty states are on the same side of the dimer row. We note that STM images are determined by both geometric and electronic effects alike. Hence, we describe the appearance in the topographies without any assumptions about the geometric structure.

For both HH and HD, the appearance in STM imaging was attributed to the formation of a single dangling bond (see Fig. 1(e)). In the case of the Si–Si–H hemihydride, the adsorption of a H atom saturates the dangling bond of one Si atom of a Si–Si dimer that would otherwise contribute to the dimer π bond [16,19]. Thus, a dangling bond is exposed on the Si atom on the opposite end of the Si–Si dimer. In the case of the Si–P heterodimer, the π bond is broken by replacing one tetravalent Si atom with a P atom with 3 bonds and a lone pair [15,24]. Such a single dangling bond was proposed to be similar to a half-filled band giving additional states for tunnelling close to the Fermi level, which leads to the elevated appearance of the dangling bond in filled and empty states STM imaging. The depression on the H and the P site of the dimer in the STM topographies were ascribed to the fact that the states of the saturated dangling bond at the hydrogen atom (HH) as well as the states of the lone electron pair of the P atom (HD) are further away from the Fermi level. According to these simple models the electronic structure near the Fermi level is essentially identical for HH and HD. Thus, it comes at no surprise that both structures have a very similar appearance in filled and empty states STM imaging and that differences will only become visible by careful comparison.

One advantage of STM-based device fabrication is that one can determine the number and precise location of dopants in the device by STM imaging. However, that requires that there is no ambiguity in appearance between intentionally placed phosphorus dopants and residual hydrogen atoms due to incomplete desorption. Our comparative STM study was thus aimed at establishing a clear experimental distinction between both features.

The results presented here consist of two parts: first, we performed an experiment with a low density both species on the surface in order to look for differences between Si–P heterodimers and Si–Si–H hemihydrides in STM imaging. Here, we first created a low density of isolated HD and then subsequently performed several dosing cycles with a small amount of atomic hydrogen at room temperature to increase the abundance of HH. A detailed survey with voltage-dependent imaging reveals subtle differences in the appearance of both features when compared directly. We assign the features in the STM images to either heterodimer or hemihydride according to their relative abundance. This finding constitutes a nice example of the power of voltage-dependent STM imaging to resolve even small differences in the local electronic structure. In the second experiment, we apply the experimental distinction of the HD and the HH to study the lateral diffusion of P atoms in the surface during a high temperature anneal out of nanoscale reservoirs created with STM lithography. Thus, we demonstrate that it is possible to monitor the P dopant distribution in the Si(0 0 1) surface during the fabrication of STM-based Si:P devices.

2. Experimental

All experiments were performed in an UHV Omicron variable temperature scanning tunnelling microscope

(VT-STM) at a base pressure of 2×10^{-11} mbar. The STM tips were etched from polycrystalline tungsten wire and outgassed for a couple of hours at 150 °C before the measurement. All STM measurements were performed at room temperature. Voltage-dependent STM images were taken simultaneously on the same surface area by switching the bias voltage when reversing the scan direction for each line.

The samples were cleaved from polished n-type Si(0 0 1) wafers doped with P to a resistivity of around 1 Ω cm. Clean Si(0 0 1) surfaces were prepared by outgassing the samples at temperatures around 550 °C for a couple of hours and flashing in UHV for 20 s at 1100 °C followed by a controlled cool-down from 900 °C to room temperature of approximately 2 K/s. The pressure during flashing and cool-down did not exceed 1×10^{-10} mbar. Atomic hydrogen was provided from cracking ultra-pure (99.9999%) molecular hydrogen on a heated tungsten filament with a water-cooled heat shroud. The PH_3 dosing was performed by opening a precision leak valve between the UHV chamber and a phosphine microdosing system. The phosphine and hydrogen doses were calibrated by counting the corresponding feature density on the surface after dosing in a separate set of experiments. Sample heating was achieved by passing a current directly through the sample. The substrate temperature was measured with an infrared pyrometer to an accuracy of ±20 K.

To prepare a Si(0 0 1) surface with heterodimers, the clean sample was dosed with typically 8.5×10^{-3} L (Langmuir) of PH_3, and annealed to temperatures of around 550 °C. Following this procedure, it is well known that the PH_3 molecules dissociate, the P atoms get incorporated into the surface, and the remaining hydrogen from the phosphine dissociation is desorbed [10–13,15]. For the preparation of isolated hemihydrides, the Si(0 0 1) sample was dosed at room temperature with typically 6.3×10^{-3} L of atomic hydrogen from a cracker cell. The hydrogen atoms randomly adsorb to individual Si atoms [16,19]. Complete hydrogen termination was achieved by heating the sample to 370 °C and exposing it to the atomic hydrogen beam for 7 min. Such a procedure routinely results in a uniform monohydride phase on the Si(0 0 1) surface [10].

3. Experimental distinction of Si–P heterodimer and Si–Si–H hemihydride

In the first experiment, we fabricated a submonolayer coverage of Si–P heterodimers on a clean Si(0 0 1) surface and then applied several subsequent small doses of atomic hydrogen at room temperature to increase the density of hemihydrides. After each step the surface was surveyed with voltage-dependent STM imaging. Thereby, we have both species present on the surface and increase the abundance of one in a controlled way. The ultimate goal was to establish an experimental distinction and assign the features to either HD or HH based on their relative abundance.

Representative voltage-dependent STM images of the surface for two of the dosing steps are shown in Fig. 2. The surface after dosing with 3.0×10^{-3} L of PH_3, followed by a 10 s anneal at a temperature of 580 °C, is shown in Fig. 2(a) and (b). It is well known that after this procedure the P atoms have incorporated into the surface, the ejected Si atoms have diffused to the step edges and the majority of the dissociated hydrogen atoms have desorbed [10–13,15].

There are a number of features on the surface appearing similar to HD or HH [11,15,16,18–24]. At a sample voltage of $U = -1.5$ V, these features appear as an asymmetric elevation on one side of the dimer. At $U = +1.5$ V, they appear as an asymmetric elevation on the dimer row with a depression on the opposite end (see enlargements). Indeed, we can distinguish two variants of these features, which we have marked A and B. As the A feature is much more abundant on the surface than the B feature, this naturally leads to identifying feature A as the heterodimer and the feature B as the hemihydride. The small amount of hemihydrides is due to incomplete desorption of the hydrogen [17].

A close inspection (see enlargements in Fig. 2(a) and (b)) reveals that feature B appears higher than feature A in both filled and empty state imaging. This becomes evident from sections of the topography data depicted in Fig. 2(c). The positions of the sections are indicated by the arrows in the enlargements of the topographic data. Imaging the filled electronic states at $U = -1.5$ V, the asymmetry of feature A and B with respect to the dimer rows is clearly visible (Sections 1 and 2). While feature B appears elevated by around 10 pm, feature A appears slightly depressed with respect to the clean Si dimers. Imaging the empty states at $U = +1.5$ V (Sections 3 and 4), the asymmetric elevation is more pronounced for feature B than for feature A.

The assignment of the features to HD or HH is corroborated in the following steps of the experiment. Subsequently, the surface was dosed with repeated cycles of roughly 6.5×10^{-3} L of atomic hydrogen at room temperature. Fig. 2(d) and (e) shows the surface after the second cycle at $U = -1.3$ V and $U = +1.3$ V, respectively (the images after the hydrogen dosing were not taken on the same surface area as the ones after PH_3 dosing and annealing). There are a number of HD/HH-like features on the surface, which can be divided into two variants A and B as before. Sections of the topographic data from these STM images for feature A and B are displayed in Fig. 2(f). While at $U = -1.3$ V both features now appear lower with respect to the surrounding clean Si dimers, again feature B is higher than feature A in both filled and empty states imaging.

After hydrogen dosing, the number of B features has clearly increased. Our identification of the HD as feature A and the HH as feature B is confirmed by a detailed surface survey after every H dosing cycle and counting statistics. Using a sampling area of more than 3200 nm^2 for each dosing cycle, we have classified the features in filled and empty states STM images into types A and B according to the description given above and determined the corre-

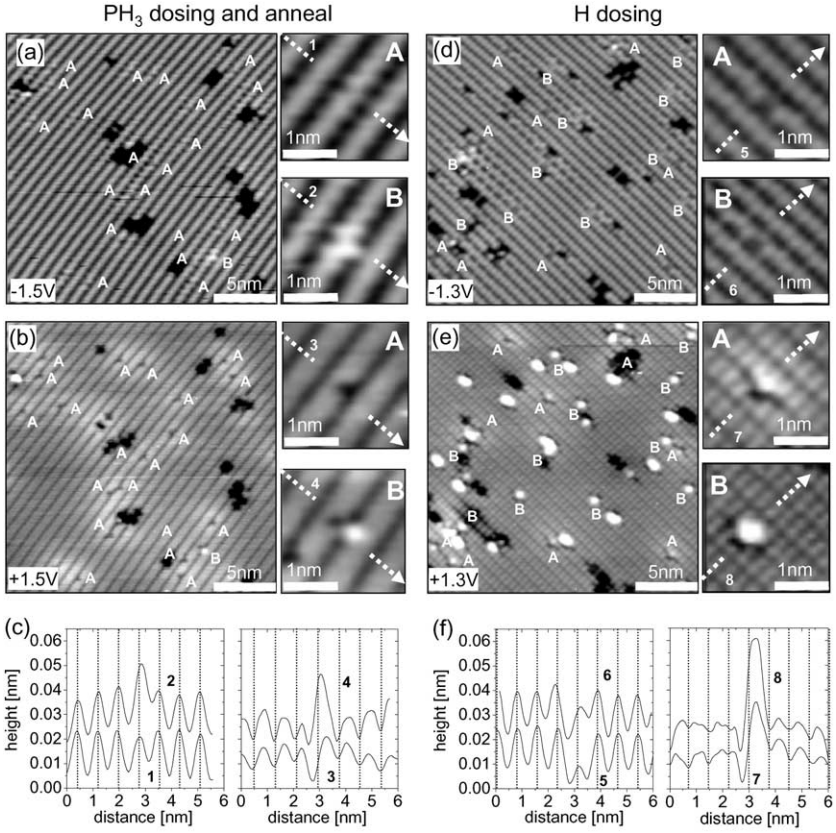

Fig. 2. Voltage-dependent STM images after dosing Si(0 0 1) with PH_3 and atomic hydrogen. (a) and (b) show the surface at $U = -1.5$ V and $U = +1.5$ V after PH_3 dosing and annealing. There are a number of heterodimer- or hemihydride-like features on the surface which exist in two different variants marked A and B (see enlargements). (c) Sections through the voltage-dependent topographies for the features A and B as indicated by the dotted arrows in the enlargements. (d) and (e) are STM images at $U = -1.3$ V and $U = +1.3$ V after subsequent dosing with approximately 0.013 L of atomic hydrogen. (f) Sections through the voltage-dependent topographies for features A and B as indicated in the enlargements. The dashed lines mark the positions of the dimer rows.

sponding surface densities (see Fig. 3). As expected, the HD density remains constant within statistical limits whereas the HH density increases by about 0.23% of a monolayer in each H dosing step. A linear fit to the HH density is shown by the solid line.

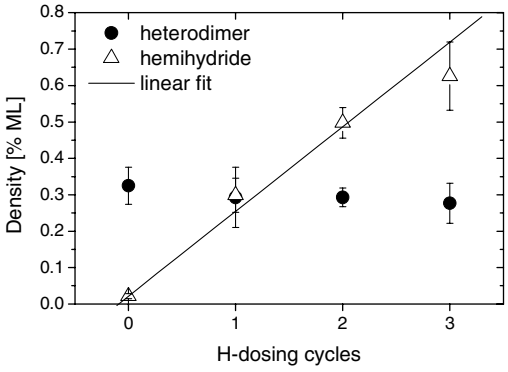

Fig. 3. Surface density of heterodimer and hemihydride features during the repeated dosing experiment. The density of the heterodimers remains constant within statistical limits whereas the hemihydride abundance increases linearly.

Comparing the data sets from Fig. 2(a) and (b) with (d) and (e) illustrates that even though the height of the features in STM imaging depends on the bias voltage and the tip condition in the experiment, the qualitative differences in the appearance between HD and HH prevail. We note that we usually survey the surface at a wide range of bias voltages and choose the tunnelling conditions giving the best distinction between HD and HH which can slightly vary from experiment to experiment.

4. Phosphorus diffusion out of nanoscale reservoirs

In the second experiment, we apply the experimental distinction presented in the previous section to determine the P diffusion out of a reservoir on the surface created by STM lithography on the hydrogen terminated Si(0 0 1):H surface [1,10,13]. Here, the adsorption of PH_3 and the incorporation of P dopants into the surface are initially restricted to the areas patterned with the STM. It is known that annealing at temperatures high enough to desorb the hydrogen will cause some lateral diffusion of the P atoms in the Si(0 0 1) surface [10,13,17]. We demonstrate that we are able to estimate the magnitude of lateral diffusion using

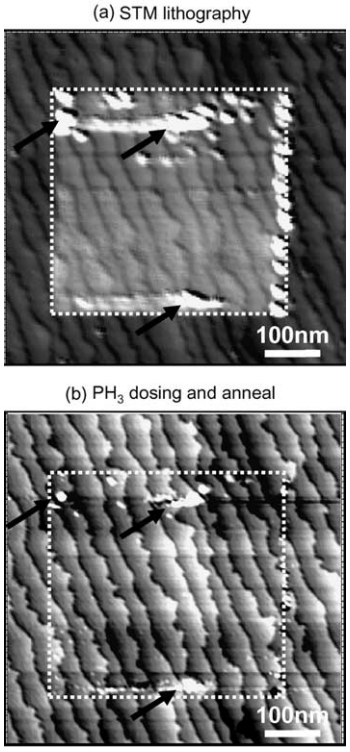

Fig. 4. STM lithography and registration to patterned areas after PH_3 dosing and annealing. (a) STM image of a patch on the Si(001):H surface patterned by STM lithography. The desorbed area appears elevated due to additional tunnelling contributions from the π states of the Si(001) surface. Marker hillocks (see black arrows) have been deposited from the tip by bias pulses. (b) The same sample area after dosing the surface with PH_3 and annealing for 10 s at 530 °C. The area of the pattern (marked by the dotted square) can be identified by the step structure as well as the marker hillocks.

the steady state P atom distribution after a high thermal anneal.

One prerequisite for determining the distribution of the phosphorus atoms in the surface with respect to the reservoir boundary is the ability to return to the same surface area with the STM tip throughout the different steps of the experiment as demonstrated in Fig. 4. Fig. 4(a) shows the hydrogen terminated Si(001):H surface with a 400 nm by 400 nm patch where the hydrogen has been desorbed by STM lithography. The patterned area appears elevated in filled states STM images due to the additional π bond states available for tunnelling on the bare Si(001) surface compared to the passivated Si(001):H surface where there are no states in the bulk band gap [1,10]. In Fig. 4(b), the sample has been dosed with roughly 0.03 L of PH_3 followed by an anneal of 10 s at 530 °C, which results in dissociation of PH_3, incorporation of the phosphorus into the surface, and desorption of the hydrogen as reported before [10–13,15]. After desorbing the hydrogen resist, the area patterned by STM lithography does not appear elevated anymore. Nonetheless, the area of the lithographic patch (marked by the dotted square) can be inferred using the underlying step structure of the Si(001) surface and by the aid of marker hillocks (see black arrows) of material deposited from the STM tip onto the surface by applying voltage pulses to the tip.

Fig. 5 shows atomically-resolved voltage-dependent STM images inside ((a) and (b)) and outside ((c) and (d)) the patterned area after phosphine dosing and annealing. Inside the patterned area, there is a high density of Si–P heterodimers and some Si–Si–H hemihydrides. In complete analogy to the previous experiment, we are able to catego-

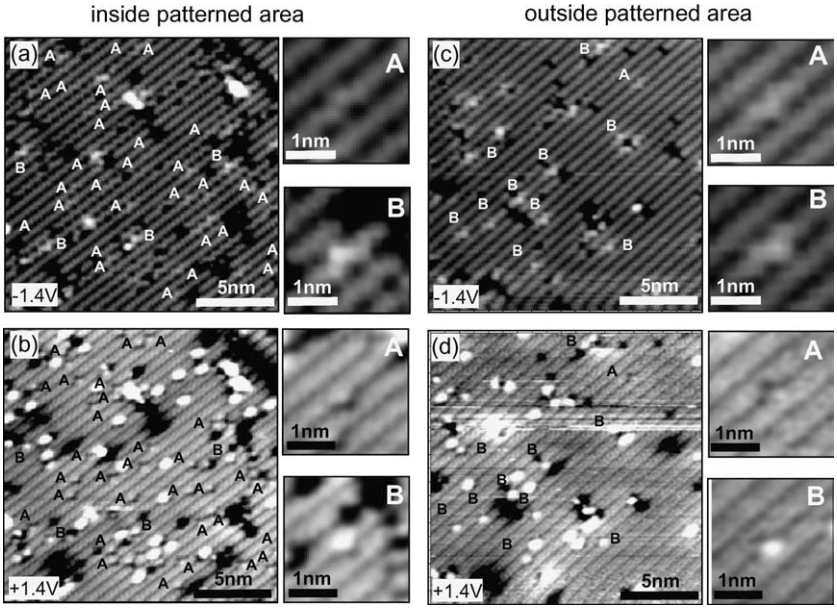

Fig. 5. Voltage-dependent STM images inside and outside a STM-patterned patch after phosphine dosing and annealing. (a) and (b) Area inside the STM-patterned area at $U = -1.4$ V and $U = +1.4$ V. (c) and (d) Area outside the patterned area at $U = -1.4$ V and $U = +1.4$ V. There is a high density of heterodimer/hemihydride features inside the patterned area and a medium density away from it. The features can be divided into two variants A and B. The asymmetric up-down appearance is more pronounced for feature B than for the A feature (see enlargements).

rize these features into type A (heterodimer) and B (hemihydride) based on their appearance in voltage-dependent imaging (see enlargements). As before, the HH appears higher in filled and empty state than the HD.

As expected, the density of Si–P heterodimers (feature A) is higher inside the area patterned with STM lithography than the density of Si–Si–H hemihydrides (feature B). Far away from the patterned area, there are mainly HH present with the occasional HD feature. The residual HH inside the lithographically defined patch (Fig. 5(a) and (b)) can arise from several sources. They can be due to incomplete hydrogen desorption by STM lithography, due to hydrogen atoms dissociated from the PH_3, or due to hydrogen atoms that have diffused from the outside into the area patterned with STM lithography during the anneal [18,23]. We assume that the HD observed far away from the patterned area are due to the occurrence of phosphine adsorption on random dangling bonds or defects in the monohydride resist layer. Furthermore, one can also see a higher density of dimer vacancies inside the patterned area compared to outside. It is well known that dimer vacancies form during annealing of the Si surface [27]. We attribute the increased formation of dimer vacancies to the relief of surface strain caused by the high phosphorus density in the areas patterned by STM lithography [17,28].

Imaging at different locations, we observe that the density of the HD does not change sharply at the border of the STM-patterned area. Instead, there is a concentration gradient as the phosphorus atoms diffuse along the surface during the thermal anneal. In order to study the P diffusion in more detail, we have analysed a series of atomically-resolved STM images on overlapping areas. The position of these scan frames with respect to the reservoir patterned by STM lithography was determined by registration of the scan offset to the same surface area as shown in Fig. 4. The concentration profile perpendicular to the border of the reservoir as extracted from the STM images are shown in Fig. 6. The HD density decreases when moving away from the patch whereas the density of the HH remains roughly constant. We estimate the diffusion constant by fitting a Gaussian concentration profile for one-dimensional diffusion with a constant total number of dopants [29] $c(x) = c_0 + a\exp(-\frac{1}{2}(\frac{x}{w})^2)$. From the width w, we calculate the diffusion length Dt via $w = \sqrt{2Dt}$ of roughly 23 nm and a diffusion constant of $D = 5.1 \times 10^{-13}$ cm^2/s at the anneal temperature 530 °C. This value is more than five orders of magnitude higher than the bulk diffusion constant extrapolated to the same temperature ($\sim 10^{-19}$ cm^2/s) [29]. The nearly constant density of hemihydrides can be explained by the rapid diffusion of hydrogen at the anneal temperature eliminating any initial concentration gradient [18,23].

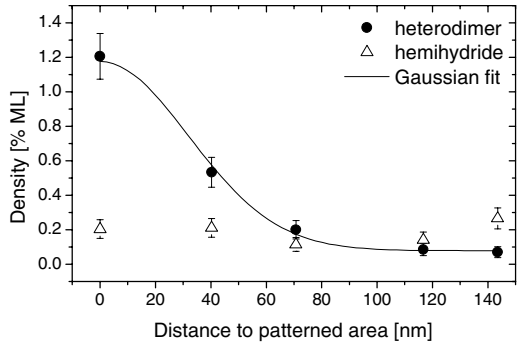

Fig. 6. Surface density of heterodimer and hemihydride as function of distance to the area patterned with STM lithography. The abundance of the hemihydride is roughly constant, whereas the decreasing density of the heterodimer reflects the surface diffusion from the patch due to the thermal anneal. The solid line depicts a Gaussian fit to the heterodimer density to estimate the diffusion length.

5. Discussion

From a close inspection of Fig. 2(b) and (d) one can see that the HD is surrounded by a circular elevation (glow) of a few nm diameter at $U = +1.3$ V which is indicative of positive charge. In contrast, the HH does not show this glow. The circular elevation around the HD arises from the effect of the screened Coulomb potential of the localised charge, which is superimposed on the periodic density of states (DOS). This electrostatic potential locally shifts the electronic bands and thereby modifies their contributions to the tunnelling current [30].

The positive charge of the HD is very likely related to states in the band gap which are depleted by the band-bending at the surface and leave a positively ionized core behind. However, the charge seems also to be dependent on the experimental conditions, as can be seen from Fig. 5(b) where the HD has no glow. The dependence on the experimental conditions can be explained by the fact that the surface Fermi level is sensitive to the overall density of surface defects as well as the electrostatic induced surface band bending of the tunnelling tip. We have observed that the visibility of the charge is reduced when the overall surface defect density is increased. Moreover, the charge is not visible at low positive bias and is best seen at medium positive sample bias (e.g. compare Fig. 1(c) with Fig. 2(b)).

The simple dangling bond model [15,16,19,24] can neither account for the different apparent height of heterodimer and hemihydride nor for the different charging of both, and therefore needs to be extended as for example by first-principles total energy and bandstructure calculations of both species.

By studying the diffusion out of nanoscale reservoirs during high temperature anneals we have demonstrated that it is possible to monitor the P distribution during the fabrication of Si:P devices by STM lithography. However, further studies are needed to obtain the temperature dependence of the diffusion, address the role of the hydrogen and surface defects, and elucidate the mechanisms of the lateral P diffusion. A promising approach would be to compare diffusion studies using the concentration profile after

diffusion—as presented here—with diffusion of single P atoms by real-time STM [27] or atom tracking STM [23,31] at elevated temperatures.

6. Conclusion

We have presented a comparative STM study on the Si–P heterodimer and the Si–Si–H hemihydride—two common surface features encountered when fabricating Si:P nanoscale devices by STM lithography. Voltage-dependent imaging reveals subtle differences in the appearance by which both features can be distinguished. The feasibility of studying the diffusion of phosphorous atoms in the Si(001) surface out of nanoscale reservoirs fabricated with STM lithography was demonstrated, obtaining a diffusion constant $D = 5.1 \times 10^{-13}$ cm^2/s at a temperature of 530 °C. The experimental distinction of the heterodimer and the hemihydride is crucial for monitoring the dopant distribution in P-in-Si nanostructures fabricated with STM lithography.

Acknowledgments

MYS acknowledges an Australian Government Federation Fellowship. This work was supported by the Australian Research Council, the Australian Government, the US Advanced Research and Development Activity, the National Security Agency and the Army Research Office under contract DAAD19-01-1-0653, and the Semiconductor Research Cooperation.

References

[1] J.W. Lyding, T.-C. Shen, J.S. Hubacek, J.R. Tucker, G.C. Abeln, Nanoscale patterning and oxidation of H-passivated Si(100)-2×1 surfaces with an ultrahigh vacuum scanning tunneling microscope, Appl. Phys. Lett. 64 (15) (1994) 2010.
[2] J.H. Cole, A.D. Greentree, C.J. Wellard, L.C.L. Hollenberg, S. Prawer, Quantum-dot cellular automata using buried dopants, Phys. Rev. B 71 (11) (2005) 115302.
[3] J.R. Tucker, T.-C. Shen, Can single-electron integrated circuits and quantum computers be fabricated in silicon? Int. J. Circ. Theor. Appl. 28 (2000) 553.
[4] T.-C. Shen, J.-Y. Ji, M.A. Zudov, R.-R. Du, J.S. Kline, J.R. Tucker, Ultradense phosphorus delta layers grown into silicon from PH_3 precursors, Appl. Phys. Lett. 80 (9) (2002) 1580.
[5] T.-C. Shen, J.S. Kline, T. Schenkel, S.J. Robinson, J.-Y. Ji, C. Yang, R.-R. Du, J.R. Tucker, Nanoscale electronics based on two-dimensional dopant patterns in silicon, J. Vac. Sci. Technol. B 22 (6) (2004) 3182.
[6] B.E. Kane, A silicon-based nuclear spin quantum computer, Nature 393 (1998) 133.
[7] D.F. Sullivan, B.E. Kane, P.E. Thompson, Weak localization thickness measurements of Si:P delta layers, Appl. Phys. Lett. 85 (26) (2004) 6362.
[8] J.R. Tucker, T.-C. Shen, The road to a silicon quantum computer, Quant. Inform. Process. 3 (1–5) (2004) 105.
[9] G. Qian, Y.-C. Chang, J.R. Tucker, Theoretical study of phosphorous δ-doped silicon for quantum computing, Phys. Rev. B 71 (4) (2005) 045309.
[10] J.L. O'Brien, S.R. Schofield, M.Y. Simmons, R.G. Clark, A.S. Dzurak, N.J. Curson, B.E. Kane, N.S. McAlpine, M.E. Hawley, G.W. Brown, Towards the fabrication of phosphorous qubits for a silicon quantum computer, Phys. Rev. B 64 (16) (2001) 161401(R).
[11] N.J. Curson, S.R. Schofield, M.Y. Simmons, L. Oberbeck, J.L. OBrien, R.G. Clark, STM characterization of the Si–P heterodimer, Phys. Rev. B 69 (19) (2004) 195303.
[12] H.F. Wilson, O. Warschkow, N.A. Marks, S.R. Schofield, N. Curson, P.V. Smith, M.W. Radny, D.R. McKenzie, M.Y. Simmons, Phosphine dissociation on the Si(001) surface, Phys. Rev. Lett. 93 (22) (2004) 226102.
[13] S.R. Schofield, N.J. Curson, M.Y. Simmons, F.J. Rueß, T. Hallam, L. Oberbeck, R.G. Clark, Atomically precise placement of single dopants in Si, Phys. Rev. Lett. 91 (13) (2003) 136104.
[14] F.J. Rueß, L. Oberbeck, M.Y. Simmons, K.E.J. Goh, A.R. Hamilton, T. Hallam, S.R. Schofield, N.J. Curson, R.G. Clark, Toward atomic-scale device fabrication in silicon using scanning probe microscopy, Nanoletters 4 (10) (2004) 1969.
[15] Y. Wang, X. Chen, R.J. Hamers, Atomic-resolution study of overlayer formation and interfaxial mixing in the interaction of phosphorous with Si(001), Phys. Rev. B 50 (7) (1994) 4534.
[16] J.J. Boland, Evidence of pairing and its role in the recombinative desorption of hydrogen from the Si(100)-2×1 surface, Phys. Rev. Lett. 67 (12) (1991) 1539.
[17] T. Hallam, F.J. Rueß, N.J. Curson, K.E.J. Goh, L. Oberbeck, M.Y. Simmons, R.G. Clark, Effective removal of hydrogen resists used to pattern devices in silicon using an STM, Appl. Phys. Lett. 86 (14) (2005) 143116.
[18] J.H.G. Owen, D.R. Bowler, C.M. Goringe, K. Miki, G.A.D. Briggs, Hydrogen diffusion on Si(001), Phys. Rev. B 54 (19) (1996) 14153.
[19] J.J. Boland, Scanning tunneling microscopy study of the adsorption and recombinative desorption of hydrogen from the Si(001)-2×1 surface, J. Vac. Sci. Technol. A 10 (4) (1991) 2458.
[20] M. Dürr, Z. Hu, A. Biedermann, U. Höfer, T.F. Heinz, Real-space study of the pathway for dissociative adsorption of H_2 on Si(001), Phys. Rev. Lett. 88 (4) (2002) 046104.
[21] Z. Hu, A. Biedermann, E. Knoesel, T.F. Heinz, Quantitative study of adsorbate–adsorbate interactions of hydrogen on the Si(001) surface, Phys. Rev. B 68 (15) (2003) 15418.
[22] J.E. Vasek, Z. Zhang, T.C. Salling, M.G. Lagally, Effects of hydrogen impurities on the diffusion, nucleation and growth of Si on Si(001), Phys. Rev. B 51 (23) (1995) 17207.
[23] E. Hill, B. Freelon, E. Ganz, Diffusion of hydrogen on the Si(001) surface investigated by STM atom tracking, Phys. Rev. B 60 (23) (1999) 15896.
[24] R.J. Hamers, Y. Wang, J. Shan, Atomic-level spatial distribution of dopants on silicon surfaces: toward a microscopic understanding of surface chemical reactivity, Appl. Surf. Sci. 107 (1996) 25–34.
[25] D.R. Bowler, J.H.G. Owen, C.M. Goringe, K. Miki, G.A.D. Briggs, An experimental-theoretical study of the behaviour of hydrogen on the Si(001) surface, J. Phys.: Condens. Matter 12 (2000) 7655–7670.
[26] E.J. Buehler, J.J. Boland, Dimer preparation that mimics the transition states for the adsorption of H_2 on the Si(001)-(2×1) surface, Science 290 (2000) 506.
[27] N. Kitamura, M.G. Lagally, M.B. Webb, Real-time observation of vacancy diffusion on Si(001)-(2×1) by scanning tunneling microscopy, Phys. Rev. Lett. 71 (13) (1993) 2082.
[28] D.-S. Lin, T.-S. Ku, C. Ru-Ping, Interaction of phosphine with Si(001) from core-level photoemission and real-time scanning tunneling microscopy, Phys. Rev. B 61 (4) (2000) 2799.
[29] S.M. Sze, Semiconductor Devices—Physics and Technology, John Wiley and Sons, 1985.
[30] G.W. Brown, H. Grube, M. Hawley, S.R. Schofield, N.J. Curson, M.Y. Simmons, R.G. Clark, Imaging charged defects on clean Si(100)-(2×1) with scanning tunneling microscopy, J. Appl. Phys. 92 (2) (2002) 820.
[31] B.S. Schwartzentruber, Direct measurement of surface diffusion using atom-tracking scanning tunneling microscopy, Phys. Rev. Lett. 76 (3) (1996) 459.